

Spatial and temporal assessment of the initial pattern of phytoplankton population in a newly built coastal reservoir

Xiangyu REN¹, Kai YANG (✉)¹, Yue CHE¹, Mingwei WANG¹, Lili ZHOU¹, Liqiao CHEN²

¹ Shanghai Key Laboratory of Urbanization and Ecological Restoration, East China Normal University, Shanghai 200241, China
² School of Life Sciences, East China Normal University, Shanghai 200241, China

© Higher Education Press and Springer-Verlag Berlin Heidelberg 2015

Abstract For decades, the main threat to the water security of a metropolis, such as the city of Shanghai, has been the rapidly growing demand for water and at the same time, the decrease in water quality, including eutrophication. Therefore Shanghai shifted the preferred freshwater source to the Yangtze Estuary and constructed the Qingcaosha Reservoir, which is subject to less eutrophic water from the Yangtze River. To assess the population of phytoplankton for the first time in the newly built reservoir, this study improved an integrated method to assess the phytoplankton pattern in large-water-area reservoirs and lakes, using partial triadic analysis and Geographic Information Systems. Monthly sampling and monitoring from 10 stations in the reservoir from July 2010 to December 2011 were conducted. The study examined the common pattern of the phytoplankton population structure and determined the differences in the specific composition of the phytoplankton community during the transition period of the reservoir. The results suggest that in all but three sampling stations in the upper parts of Qingcaosha Reservoir, there was a strong common compromise in 2011. The two most important periods occurred from late summer to autumn and from winter to early spring. The former was characterized by the dominance of cyanobacteria, whereas the latter was characterized by the dominance of both chlorophyta and diatoms. Cyanobacteria (*Microcystis* spp. as the main genus) were the monopolistic dominant species in the summer after reservoir operation. The statistical analysis also indicated the necessity for regular monitoring to focus on the stations in the lower parts of the reservoir and on several limited species.

Keywords phytoplankton dynamics, Partial Triadic Analysis, Geographic Information Systems, management, Qingcaosha Reservoir, Shanghai

1 Introduction

In the context of a threat to water security, reservoirs are considered worldwide to be a preferred or additional water supply resource. Many new reservoirs have been constructed, and the capacities for several existing reservoirs have been enlarged (Dudgeon, 2000; Pringle, 2001; Zeng et al., 2007; Kummu, 2009). However, the waters of some inland lakes and freshwater reservoirs have been experiencing eutrophication, which consequently increases the frequency of phytoplankton blooms and changes the structure of the biological network (Bartram et al., 1999). This change has resulted in the health risk of microcystin in drinking water. Thus, eutrophication and phytoplankton proliferation are among the most critical problems in reservoir operation, especially in the tropics and subtropics.

Complicated reasons for eutrophication and its impact on phytoplankton were researched. The major concern of eutrophication is that the nutrient concentration (both from known point sources and sediments) is strongly and positively correlated with phytoplankton blooms in lakes, estuaries and harbors (Schindler, 1977; Smith, 1983; Downing et al., 2001; Pinckney et al., 2001; Chau and Muttill, 2007; Zeng et al., 2007). Other studies have shown that additional factors, such as the flow rate, tidal amplitude, meteorological factors, and water column mixing in rivers or lakes, may have a greater effect on phytoplankton than nutrients (Maier et al., 2012). Further studies have revealed that variations in the phytoplankton composition in reservoirs are strongly related to the reservoir characteristics, such as grazing, retention time, depth, and water quality (Hunt and Matveev, 2005;

Karadžić et al., 2010; Soares et al., 2012). Furthermore, some researchers focused on predicting the algae bloom by applying statistical methods, such as genetic programming and an artificial neural network (Muttill and Chau, 2006, 2007).

Subjected to rapid urbanization and a population explosion, Shanghai, the largest metropolis of China, is faced with serious water security threats. One threat is the inadequate water supply. Until 2009, the water supply of Shanghai was 9.75×10^6 m³/d, much less than the water demands of the entire city. Therefore, the government needed to increase output to meet water demands. Water quality deterioration, including eutrophication, posed an additional threat. In 2009, more than 80% of Shanghai's water supply was pumped from the Huangpu River (Shanghai Water Authority, 2009), located in the lower reaches of the Tai Lake basin. Unfortunately, these waters had experienced serious eutrophication problems (Chen et al., 2003a,b; Pan et al., 2011). The phytoplankton bloom in Tai Lake in the summer of 2007 caused a mass panic resulting in an increased public interest in cyanobacteria bloom found in drinking water resources (Ren et al., 2010). Since that time, water quality and eutrophication from upstream has become a serious threat to the water supply of Shanghai.

Comparatively, the water from the Yangtze Estuary is superior in both quality and quantity. Data from the Shanghai Environmental Monitoring Center demonstrated that the water quality in the Yangtze Estuary has been relatively high and remained stable for over 10 years. Most indicators met the national standards for water protection zones of surface drinking water sources (Grade II of the Environmental Quality Standards for Surface Water of China (GB3838-2002)). Given the above considerations, Shanghai changed its preferred freshwater resource from the Huangpu River to the Yangtze Estuary and constructed the Qingcaosha Reservoir in the watercourse of the Yangtze Estuary. The reservoir started a test run in December 2010 and has been in regular operation since June 2011. However, eutrophication in the Yangtze Estuary and the near coastal area has been increasing as observed through further chemical analysis over a long time period. The concentrations of dissolved inorganic nitrogen (DIN) and dissolved inorganic phosphorus (DIP) increased from 18.4 and 0.22 $\mu\text{mol/L}$ in 1955 to 124 and 1.42 $\mu\text{mol/L}$ in 2008, respectively (Dai et al., 2011). The increasing trend is ongoing; for example, total nitrogen (TN) and total phosphorus (TP) increased to 4.48 mg/L and 0.34 mg/L, respectively, in 2010 (Chen et al., 2012). If the Carlson Trophic State Index (CTSI) is considered, the water in this area is classified as eutrophic (Carlson, 1977). Rapid urbanization and environmental degradation in the upper Yangtze River basin and the delta region are responsible for the increasing urban and agricultural pollution input of nutrients in the Yangtze Estuary.

Therefore, the nutrient concentration is not expected to decrease in the near future.

In this regard, the Qingcaosha Reservoir is still at risk for a phytoplankton bloom. Therefore, the first assessment of the initial biomass of phytoplankton is in high and urgent demand. Sampling and monitoring at 10 sampling stations was conducted monthly in the Qingcaosha Reservoir during the construction period, the operational testing period, and also during the first several months of regular operation. Phytoplankton species were artificially identified and counted to obtain access to detailed data for further analysis. The study then improved on an assessment method by combining Geographic Information Systems (GIS) and statistical method partial triadic analysis (PTA) to reveal the common pattern of the population and the characteristic temporal period in the operation of reservoir, and to check the statistical results as well as the general pattern and special case scenarios. The consequent advice in the adaptive management of the reservoir and the lake was provided based on the statistical analysis. The main highlights of this study include: (i) an improvement of the assessment method through the integration of the GIS method and the PTA method for phytoplankton population management in large-water-area reservoirs; (ii) a statistical analysis of the biomass and the spatial distribution pattern of the phytoplankton population in the entire reservoir; and (iii) a discussion of possible reservoir management and early warning measurements.

2 Study area

The Yangtze Estuary is the lower, tide-affected section of the Yangtze River. The local climate is subtropical monsoon with four distinct seasons and plenty of rain and sunshine. The annual mean temperature is 15.0°C–15.8°C, with January and February as the coldest months, and July and August the warmest. The annual mean precipitation is 1,000–1,100 mm. The estuary is composed of three stages and four outlets entering the East China Sea. The Qingcaosha Reservoir is located in the watercourse of the north channel, northeast of the Shanghai urban center. It mainly includes two intertidal wetlands: the Center Sandbar and the Grass Sandbar (Fig. 1). The total area of the reservoir is 70.46 km² and the effective capacity is 4.3×10^8 m³. The active elevation is controlled at 7 m or below during the salt-tide period and from 2 m to 4 m during the non-salt-tide period. The elevation under regular operation is controlled at 2.7 m and is presently the largest coastal reservoir of Asia. The water flow in the reservoir has been enhanced by draining through the sluice downstream. Synchronous water quality monitoring was conducted by the Shanghai Controlling and Monitoring Center of Water Supply and indicated an appropriate habit with a relatively high nutrient concentration. The annual average

concentrations of TN and TP are 1.50 mg/L and 0.07 mg/L, respectively. This enormous water area and relatively shallow water level make the Qingcaosha Reservoir an ideal habitat for phytoplankton to proliferate. In addition, the reservoir is an appropriate case for the integrated assessment method study.

3 Materials and methods

3.1 Sampling and phytoplankton analysis

To obtain enough data of the initial phytoplankton community in the newly built reservoir, samples were collected monthly from July 2010 to December 2011, which covered the construction period, test operation period, and first several months of regular operation. Ten sampling stations were distributed evenly from the inlet sluice to the outlet sluice in the east-west elongated reservoir. Stratified 1-L samplings were conducted at every station using a 5-L Van Dorn bottle and fixed by Lugol's iodine solution immediately for phytoplankton enumeration. The samples were maintained for 24 hours, and then, the supernatant, approximately 500–700 mL for each sample, was removed using the siphon method. The remaining contents were then statically maintained for another 24 hours. After these initial 48 hours, each sample was concentrated to 30–50 mL for further identification and enumeration. To classify phytoplankton into species and avoid the bias caused by transparency and suspended solids in the water, the artificial hemocytometer counting method was applied. The final volume of each sample was recorded for the biomass calculation. Then, 0.1 mL of concentrated sample was immediately drawn into the pipette after mixing. A counting slide with a grid area of 20×20 mm² was then filled. Finally, for each counting slide, the phytoplankton in 100 microscopic fields would be counted. Each sample was counted twice for 100 total scopes each. If the difference between the two counting

methods was more than 15% of the average amount, a third counting was conducted and the average was used as the reported value. All of the identifications and enumerations of the algae species were performed using a hemocytometer counting method on a MoticBA410 microscope (Motic China Group Co., Ltd.) at high magnification (×400). Meanwhile, for more accurate phytoplankton identification, qualitative samples were collected through plankton net with a pore size of 64 μm, and the resultant samples were stored in sampling bottles without preservatives to maintain the photosynthetic pigment.

Because the biomass and species before and after regular operation were markedly different, the 2011 data were analyzed to reveal the phytoplankton dynamic pattern. Data from 2010 were used for a comparison of the variation tendency. Some rare species emerged in merely one or two months and only in some stations during the monitoring, for example, *Ceratium* spp. and *Tribonema* spp. These data will assist in explaining the detailed population evolution. They will also add outliers in the modeling calculation, which will complicate the common compromise matrix. Therefore, regarding the representation of the results, 39 out of 335 species identified in the survey were selected and analyzed (Table 1). The selection was based on the following two constraints: 1) each selected species was required to show up in all ten sampling stations during each sampling month, and 2) the biomass of each selected species represented more than 0.1% of the total phytoplankton biomass.

3.2 Integrated assessment method

An integrated assessment method was improved to analyze the phytoplankton population and distribution patterns in the entire area of large lakes and reservoirs. The first step was to statistically calculate the common pattern when the same variables were assessed at the same sampling stations over a series of sampling dates using the partial triadic analysis method. The second step was to determine the

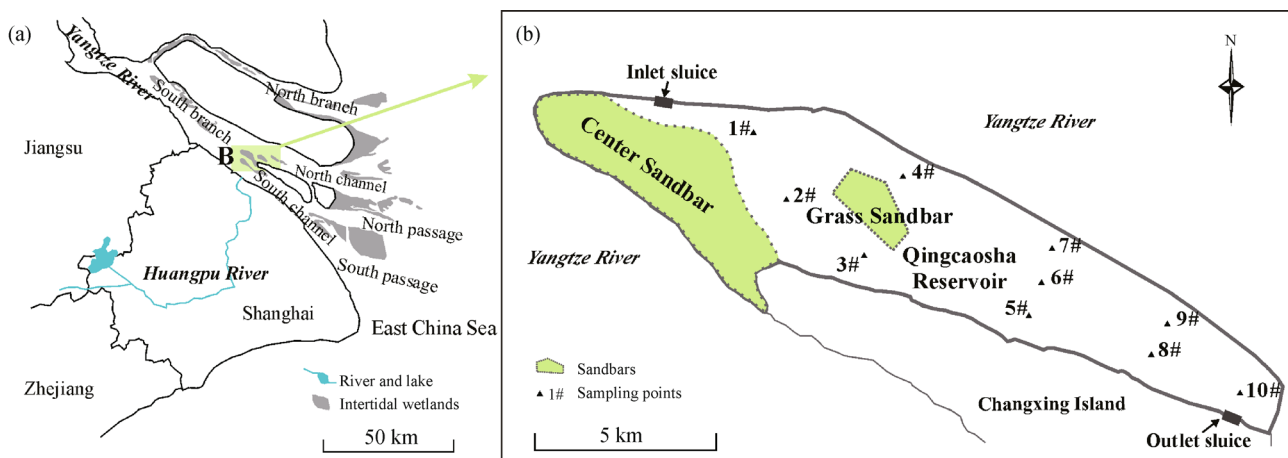


Fig. 1 Location of the study area and monthly sampling stations.

Table 1 Thirty-nine species, representing over 0.1% of the total phytoplankton abundance

Cyanobacteria		Chlorophyta		Diatoms		Cryptophyta	
No.	Species	No.	Species	No.	Species	No.	Species
1	<i>Microcystis</i> spp.	3	<i>Scenedesmus quadricauda</i>	15	<i>Melosira ambigua</i>	4	<i>Chroomonas acuta</i>
2	<i>Phormidium tenne</i>	5	<i>Chlorella vulgaris</i>	17	<i>Cyclotella</i> spp.	11	<i>Cryptomonas erosa</i>
7	<i>Chroococcus</i> spp.	6	<i>Ulothrix</i> spp.	21	<i>Synedra acus</i>	34	<i>Cryptomonas ovata</i>
		8	<i>Tetraëdron trilobulatum</i>	22	<i>Leptocylindrus danicus</i>	36	<i>Cryptomonas obovata</i>
		9	<i>Nephrocystium agardhianum</i>	24	<i>Synedra ulna</i> var. <i>angustissima</i>		
		10	<i>Scenedesmus bijuga</i>	25	<i>Hyalodiscus subtilis</i>		
		12	<i>Ankistrodesmus falcatus</i>	31	<i>Synedra vaucheriae</i> var. <i>capitellata</i>		
		13	<i>Crucigenia quadrata</i>	32	<i>Synedra affinis</i> Kütz		
		14	<i>Goelastrum microporum</i>	37	<i>Fragilaria capucina</i>		
		16	<i>Chlamydomonas</i> spp.				
		18	<i>Hormidium kützing</i>				
		19	<i>Kirchneriella lunaris</i>				
		20	<i>Oocystis lacustris</i>				
		23	<i>Schroederia</i> spp.				
		26	<i>Westlla botryoides</i>				
		27	<i>Chlamydomonas globosa</i>				
		28	<i>Oocystis</i> spp.				
		29	<i>Crucigenialauterbornii</i>				
		30	<i>Selenastrum capricornutum</i>				
		33	<i>Tetraedron minimum</i>				
		35	<i>Ankistrodesmus angustus</i>				
		38	<i>Chlorella ellipsoidea</i>				
		39	<i>Scenedesmus dimorphus</i>				

phytoplankton biomass and present the distribution using the GIS method.

PTA is a multivariate data mining method that is applied for the analysis of data arrays recorded through a series of samplings. Unlike principal component analysis, which focuses on the relationship between parameters, PTA allows one pattern that is common to all matrices representing different areas in the reservoir to be identified and the spatial differentiation in the reservoir to be clarified. The application of PTA to solve analysis problems involving spatial-temporal variations of species distributions in ecology has been previously presented (Pavoine et al., 2007). To date, PTA has been applied to several ecological studies, such as those on fish and cephalopod assemblages, the spatiotemporal patterns of earthworm communities, and the composition of larval and juvenile fish assemblages (Gaertner, 2000; Rossi, 2003; Carassou and Ponton, 2006). However, there have been few applications of PTA in phytoplankton ecology. Rolland et al. (2009) applied PTA to a dataset of phytoplankton in the Marne Reservoir to identify dynamic patterns. Bertrand and Maumy (2010) elaborated on the

calculation method, which led to new directions in PTA research. The first step is an inter-structure analysis, which corresponds to a general situation and calculates the weight of each matrix. The second step is the computation and analysis of the compromise matrix, which is the weighted mean of the series of sampling data. The final step explores the differences between the common structure and the series of sampling data (Rossi, 2003; Bertrand and Maumy, 2010). The first two steps were applied in this study. The variability of the compromise matrix and other sampling data were presented using the clustering analysis method (Legendre and Fortin, 1989; Thomas et al., 2010). All of the data were analyzed using R software (version 2.14.2).

After the sampling matrix of the different sampling months were projected onto the first eigenvectors axis resulting from the compromise matrix, the most representative sampling periods were determined and chosen for the spatial assessment. The phytoplankton biomass data from these sampling months were then applied to the sampling stations along with the latitude and longitude of the stations. The outlines of the sandbars in, and the embankment of, the Qingcaosha Reservoir were set as the

analysis mask for spatial analysis. The embankment was also set as the analysis extent for the output of the map. Based on the sampling data in each sampling station, a simulation of the spatial distribution of the entire reservoir using the Inverse Distance Weighted method was applied in the Interpolate to Raster analysis (Garant et al., 2005). The distribution and change of each raster during the same months in 2011 and 2010 were then compared with the statistical common pattern from the former analysis. All the data and spatial analysis were executed using the widely recognized and applied geographic information software ArcGIS (Version 9.3) from the Esri Company (Roberts et al., 2010).

4 Results

4.1 Analysis between the sampling stations

In regard to the structure of the phytoplankton community, the scatter diagram shows the similarities between 10 sampling stations (Fig. 2). The first eigenvalue was isolated from the others and represents 76.04% of the total inertia (Fig. 2(b)); the following analysis focused on the first Euclidean space. Overall, all 10 sampling stations had a high value on the first axis, indicating a strong common spatial structure shared in the different regions of the Qingcaosha Reservoir. The separation of the distribution on the second axis emphasized the differences in the annual phytoplankton structure between the 10 sampling stations. The structure was basically distributed into two groups: one including the first four stations located in the upper part of the reservoir and another including the stations near the sluice at the lower part of reservoir (Fig. 2(a)).

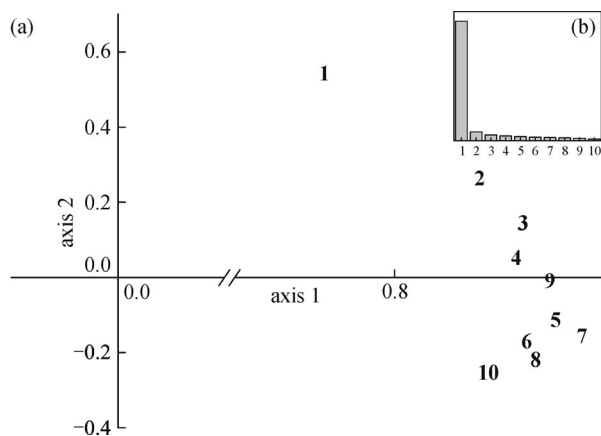


Fig. 2 Inter-structure analysis: (a) coordinates of the 10 stations given by the first two eigenvectors; (b) eigenvalue histogram.

between the sampling stations. The RV coefficient was first utilized by Robert and Escoufier (1976) and is also known as Escoufier's RV-coefficient and as a congruence coefficient. This classical Pearson correlation coefficient, between 0 and 1, represents similarity between two matrices. The closer the RV coefficient of two matrices is to 1, the more similar the association between the two. Based on the RV coefficient between the stations, the strongest correlation was found between station 5 and station 7 (RV coefficient = 0.829, which is close to 1) and the weakest was found between station 1 and station 10 (RV coefficient = 0.566). One preliminary finding is that Euclidean distances were shorter for stations 5, 6, 7, and 8, whereas these distances were longer between stations 2 and 3 and the former stations.

When the compromise matrix was concluded with a sub-matrix of 10 sampling stations, the contribution of 10 sub-matrices in constructing the compromise matrix could be expressed by the coefficients X_n , where n represented the sampling station number. These coefficients represented the weight of each sub-matrix in the calculation of the compromise matrix within a range of 0 and 1. The compromise was represented by the sum of the multiplied result of each sub-matrix and its weight coefficient for each of the eigenvectors. The nearer the weight was to 1, the more information of the corresponding sub-matrix would be kept in the compromise. The weight coefficients of Stations 7, 5, and 9 were the largest at 0.333, 0.327, and 0.325, respectively, while Stations 1 ($X_1=0.274$) and 2 ($X_2=0.309$) had the lightest weights (Table 2). Therefore, it can be concluded that the stations in the middle-to-lower part of the reservoir contributed more strongly to the overall annual phytoplankton structure. The weight also indicated how much of each station's information was included in the compromise. Thus, it could be presumed that the compromise contained more information from stations 7, 5, and 9 and less from stations 1 and 2. Because the lower part of the reservoir was expressed more in the compromise, the analysis of the compromise described the patterns corresponding to the waters of the lower region, near the sluice. The state of water quality and phytoplankton in this region had a direct bearing on the operation of the reservoir.

4.2 Analysis of the compromise

The compromise featured 39 rows and 12 columns, as shown by Table 3. It expressed the spatially stable part of the annual structure of the phytoplankton community in the reservoir. With 28.36% for axis 1, 23.13% for axis 2, and 11.65% for axis 3 (Fig. 3), the first three eigenvalues accounted for over 60% of the total inertia structure. As in other studies, this percentage of the first three eigenvalues was only slightly greater than 50% (Rossi, 2003; Rolland et al., 2009). Given that the 39 species selected were most responsible for the observed situation, an analysis of the

The left column of Table 2 presents the "RV coefficient"

Table 2 Correlations between the matrices of compromise and 10 sampling stations

Weight	1	2	3	4	5	6	7	8	9	10	Compromise
0.274	1	0.676	0.676	0.631	0.605	0.577	0.635	0.607	0.677	0.566	0.749
0.309		1	0.762	0.783	0.724	0.715	0.721	0.689	0.731	0.647	0.848
0.319			1	0.744	0.820	0.748	0.751	0.698	0.770	0.701	0.874
0.318				1	0.740	0.772	0.783	0.728	0.733	0.716	0.878
0.327					1	0.794	0.829	0.821	0.777	0.717	0.904
0.320						1	0.798	0.793	0.738	0.741	0.882
0.333							1	0.824	0.815	0.814	0.917
0.322								1	0.784	0.781	0.888
0.325									1	0.785	0.894
0.311										1	0.858

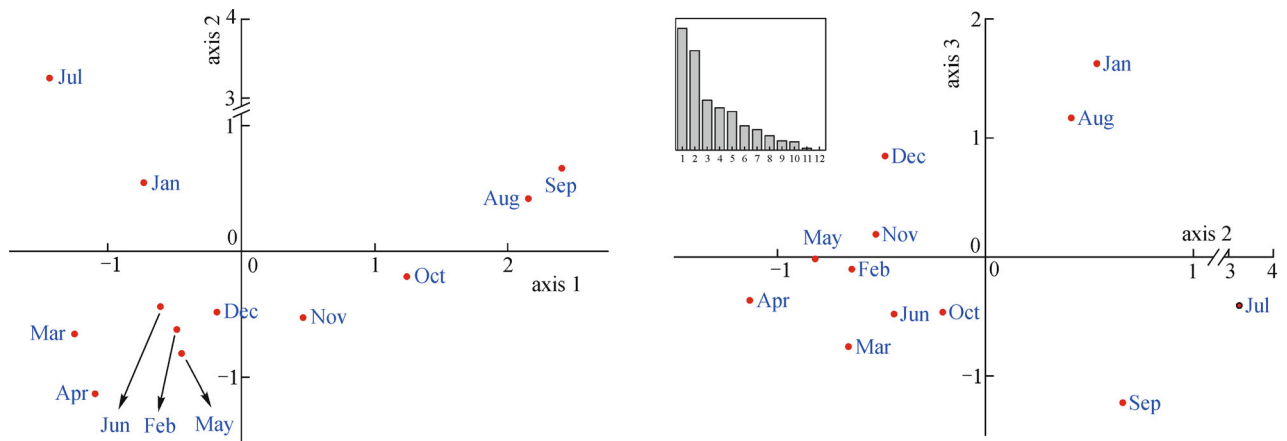


Fig. 3 Coordinates of the sampling dates in the first two planes of the compromise.

first three eigenvalues could provide a convincing summary of the temporal species organization over 10 stations during one year.

If the sampling data for each month was projected onto the axis, a conclusion about the contribution of each time period to the whole pattern would be revealed as a visual perception interpretation of the compromise (Fig. 3). The first axis of the compromise analysis was defined by two distinct periods: one in the negative part of the first axis related to winter and spring (December to February and March to May) and one related to late summer and autumn (August to November), which contributed significantly to the positive direction. During this period of time (the time periods with significant projections on the first axis), the phytoplankton population characteristics were considerably distinct from those during other times. Additionally, the phytoplankton population appeared to proliferate greatly (this will be discussed later). This proliferation resulted in a risk of the water supply because of the subsequent microcystins. Therefore, the time period from

August to November could be identified as the key period in the Qingcaosha Reservoir. These findings reveal the main temporal pattern in the reservoir. The second and third axes show the differences between the months in the period represented by the positive part of axis 1. August and September are in the positive direction of axis 2, whereas October and November are in the negative direction. The small differences between the time periods of December to January and of February to June are shown by axis 3, and constitute a second phytoplankton growth period (second to that in late summer to autumn).

A species analysis showed that these projections form two groups (Fig. 4). The first group, which included cyanobacteria, cryptophyta, and a few species of chlorophyta, occurs in the positive part of the first axis. This group represents the main species in the key period of August to November: *Microcystis* spp., *Phormidium tenne*, and *Chroococcus* spp. for cyanobacteria; *Chroomonas acuta*, *Cryptomonas erosa*, *Cryptomonas ovate*, and *Cryptomonas obovata* for cryptophyta; and *Tetraëdron*

Table 3 Transposition of the matrix of compromise

No.	[1,]	[2,]	[3,]	[4,]	[5,]	[6,]	[7,]	[8,]	[9,]	[10,]	[11,]	[12,]
1	-1.616	-1.772	-1.772	-1.772	-1.772	0.849	5.280	1.600	4.592	-0.173	-1.681	-1.762
2	-1.039	-1.039	-1.039	-1.039	-1.039	-1.039	-1.039	-1.002	8.577	-0.429	1.019	-0.890
3	7.940	-1.465	-1.350	-1.136	-0.780	-0.509	2.716	-1.069	-1.213	-1.318	-1.042	-0.774
4	0.204	-0.066	2.234	1.166	1.783	1.232	-2.351	-1.180	2.314	1.310	-3.431	-3.214
5	1.341	-1.554	7.103	-0.875	-0.581	0.785	1.908	-2.555	-0.818	-1.591	-1.409	-1.751
6	-1.731	-1.387	-1.014	-1.731	-0.202	5.898	3.118	-1.297	0.642	-1.382	-0.847	-0.067
7	-1.248	-1.248	-1.150	-1.244	-1.248	-1.248	-0.335	5.021	5.299	-0.102	-1.248	-1.248
8	-1.422	-1.422	-1.422	-1.422	-1.422	-1.422	-1.422	2.840	3.459	6.280	-1.306	-1.323
9	-0.017	-1.239	-1.665	-1.524	-1.654	-1.257	7.745	0.023	1.205	1.289	-1.566	-1.340
10	-0.370	-1.454	-1.477	-1.477	-1.477	-1.477	-1.477	9.158	0.569	-0.899	-0.209	0.591
11	-1.088	-1.741	1.369	-1.655	-1.091	-0.103	-1.767	0.431	3.298	0.101	3.023	-0.776
12	-0.394	-1.306	3.137	8.828	-1.181	-1.339	-1.100	-1.361	-1.361	-1.361	-1.302	-1.260
13	2.324	-1.776	-1.776	-1.776	-1.776	-1.776	1.442	3.742	-0.738	-1.591	1.108	2.593
14	3.582	-1.036	-0.890	-1.447	-1.313	-0.848	3.638	-0.685	2.806	-0.912	-1.447	-1.447
15	-1.175	0.041	2.855	2.954	2.031	2.133	1.888	-2.208	-2.208	-2.208	-1.897	-2.208
16	0.095	-0.979	0.249	-0.403	-0.946	-1.232	8.453	-1.378	-1.378	-1.378	-0.984	-0.120
17	-2.130	-2.491	-1.790	-2.158	-1.738	-1.840	0.969	5.830	1.856	0.777	1.585	1.132
18	-1.220	-1.220	-1.220	-1.220	-1.220	-1.220	-1.220	0.242	4.727	-0.675	4.086	0.164
19	1.066	-2.046	0.132	0.577	-2.046	0.971	4.824	0.255	0.373	-0.501	-1.684	-1.921
20	6.339	-1.642	-1.500	-1.289	-0.255	-0.947	-0.714	1.214	2.497	-0.615	-1.682	-1.405
21	-1.172	-0.523	8.082	2.345	-1.721	-1.952	-1.298	-0.247	-0.929	-1.837	-1.240	0.492
22	1.353	-1.135	-0.184	-1.135	-1.135	-1.135	-1.135	3.856	3.328	-0.565	-1.135	-0.977
23	7.797	-0.907	-0.924	-0.924	-0.924	-0.924	1.430	-0.924	-0.924	-0.924	-0.924	-0.924
24	-1.084	-1.084	-1.084	-1.084	-1.084	-1.084	-1.084	8.411	-0.300	1.649	-1.084	-1.084
25	-1.327	-1.327	-1.327	-1.327	-1.327	-1.327	-1.327	1.654	4.794	2.664	0.965	-0.785
26	3.776	-1.406	2.609	-0.210	-0.863	-1.406	4.529	-1.406	-1.406	-1.406	-1.406	-1.406
27	-1.396	-1.080	-1.775	-1.008	2.150	-0.476	-1.775	-1.131	1.463	-0.078	5.994	-0.887
28	-1.080	-1.080	-0.388	-1.080	-1.080	-0.026	9.077	-1.080	-1.080	-1.080	-0.125	-0.976
29	3.634	-1.311	-0.452	-0.843	-1.180	-1.311	-1.032	-1.311	-1.311	-1.311	0.750	5.677
30	-0.345	-1.611	-1.611	-1.432	-1.470	-1.611	7.143	1.829	-1.372	-0.410	0.061	0.831
31	-1.586	-1.319	4.453	1.061	-1.586	4.616	-1.586	0.843	-0.530	-1.312	-1.468	-1.586
32	-0.381	-0.399	1.690	-1.058	-1.345	-1.012	6.996	-1.345	-0.275	-1.345	-0.863	-0.662
33	-1.504	-1.504	-1.504	-1.504	-1.504	-1.504	-1.504	1.983	4.494	4.468	0.869	-1.284
34	0.111	1.137	-0.583	-0.912	-0.910	-1.055	1.192	1.223	2.687	0.563	-1.726	-1.726
35	-0.771	-0.737	-1.204	8.201	-1.060	-1.204	-0.659	-1.204	-1.204	-1.204	-0.807	1.853
36	-1.441	-1.441	-1.441	-1.441	-1.441	-1.441	-1.441	1.515	5.226	3.586	0.412	-0.654
37	-1.424	2.034	-0.406	-0.329	-1.424	-1.424	7.008	-1.424	1.530	-1.424	-1.292	-1.424
38	-1.192	-1.099	-1.192	-1.192	-1.192	-1.005	-1.192	-0.551	6.691	4.259	-1.145	-1.192
39	-0.193	-1.083	-1.083	-0.133	-1.083	-1.083	-1.083	6.821	2.165	-1.083	-1.083	-1.083

trilobulatum, *Scenedesmus bijuga*, *Crucigenia quadrata*, *Hormidium kützing*, *Oocystis lacustris*, *Chlamydomonas globosa*, *Chlorella ellipsoidea*, and *Scenedesmus dimorphus* for chlorophyta. Some species of diatoms (*Hyalodiscus subtilis*, *Cyclotella* spp., *Leptocylindrus danicus*

and *Synedra ulna* var. *angustissima*) also belong to this group. These species were observed more often in summer and autumn than other species. The second group, involving most species of chlorophyta (*Scenedesmus quadricauda*, *Chlorella vulgaris*, *Ulothrix variabilis*,

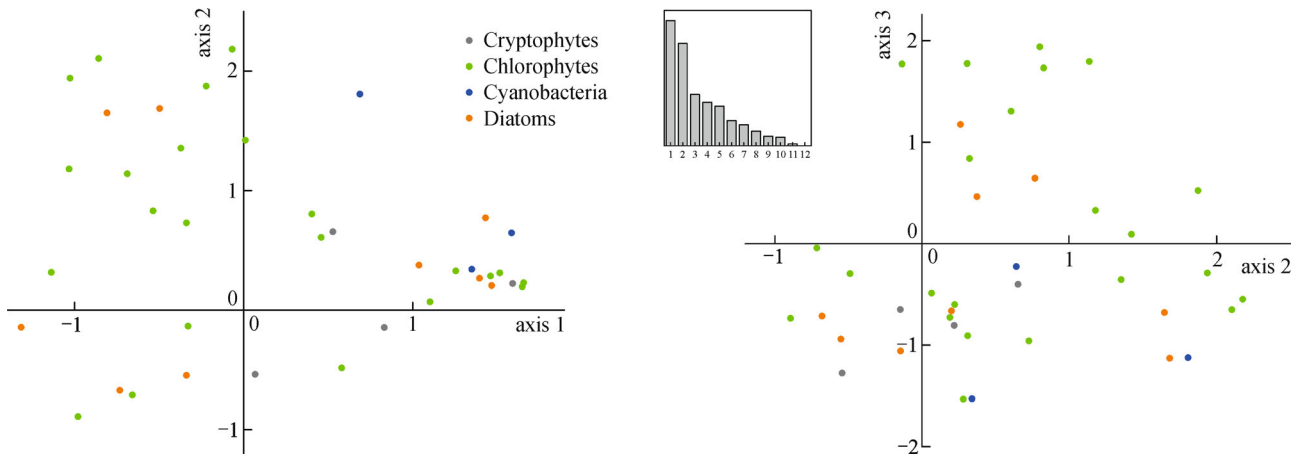


Fig. 4 Projection of the species in the first two planes of the compromise matrix.

among others) and diatoms (*Melosira ambigua*, *Synedra acus*, *Synedra vaucheriae* var. *capitellata*, *Synedra affinis* Kütz, and *Fragilaria capucina*) occur in the negative direction of axis 1. These species mainly dominate the community in the winter and spring.

The second and third axes reveal the small differences in the phytoplankton population between months: one represented winter and the other represented spring to early summer. The first assembly primarily contained species, such as *Scenedesmus bijuga* and *Scenedesmus quadricauda*, which were observed in winter. The second assembly contained *Ankistrodesmus falcatus*, *Chlamydomonas globulosa*, and *Ulothrix* spp., which were more frequently observed in the spring.

The dominance index (defined as Y) of each species of phytoplankton revealed its relative dominance. McNaughton's dominance was applied in the analysis to obtain the monthly calculation result. The dominant species from August to November were *Microcystis* spp. and *Chroococcus* spp. for cyanobacteria, *Tetraëdron trilobulatum* and *Scenedesmus bijuga* for chlorophyta, and *Fragilaria capucina* and *Cryptomonas erosa*. The dominant species in the Qingcaosha Reservoir from December to May were *Scenedesmus quadricauda*, *Chlorella vulgaris*, *Ulothrix* spp., *Melosira ambigua*, *Cyclotella* spp., and *Fragilaria capucina*. This result supported the analysis of the compromise matrix.

In summary, two time periods were most relevant for studying phytoplankton in the Qingcaosha Reservoir. The sampling date projection revealed two main assemblies: one from late summer to autumn (August to November) and one from winter to spring. By combining the biomass and the dominance index, the species composition in each period was found to be different and therefore characteristic.

4.3 Analysis of the spatial distribution and similarities

When comparing the structure of the compromise and

datasets from the 10 sampling stations, the first step was to centralize the compromise matrix. The correlations between the matrices of the compromise and 10 sampling stations could then be calculated (presented in Table 2). Between the compromise and the various sampling stations, the strongest correlation occurred at station 7 (RV coefficient = 0.917) and the weakest at station 1 (RV coefficient = 0.749). The high RV correlations implied that small spatial differences still existed despite the strong common pattern in the reservoir as a whole.

A tree topology was utilized to illustrate the spatial similarities in the different regions of the reservoir (Fig. 5). Stations 5–10 seemed to be linked as one group with patterns similar to that of the compromise matrix for the entire reservoir. Stations 2–4 defined a different group with a larger Euclidean distance from the compromise than the other group. This classification indicated that Station 1 was different from the others and from the compromise of the entire reservoir.

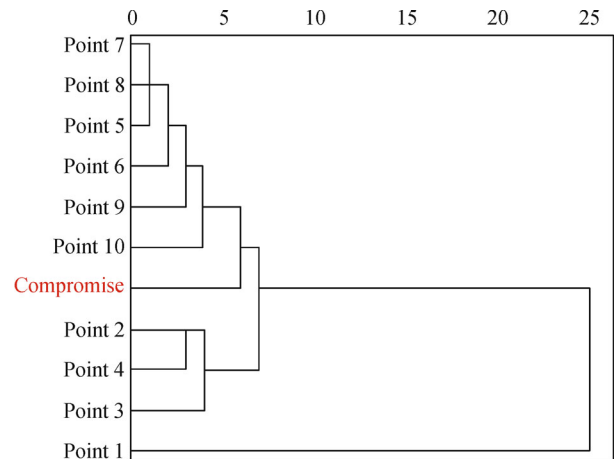


Fig. 5 Tree topology obtained by the hierarchical cluster method indicating the classification of the datasets of 10 sampling stations and the compromise.

The monthly sampling projections in the compromise showed that August, September, and October made the most significant contribution on the first eigenvectors axis in the positive direction (Fig. 3). Therefore, the samples in these months represent the common pattern for the entire temporal perspective. Moreover, in August, September, and October of 2011, the biomass of phytoplankton, including cyanobacteria and chlorophyta, the major components of the phytoplankton population, experienced a significant increase. Thus, a GIS-based assessment was introduced into the sampling data of these three months of 2010 and 2011, showing an increased biomass of each region in the reservoir (Fig. 6). The different hues indicate the degrees of proliferation one year after the construction of the reservoir, while the deeper the hue, the greater the increase. Most apparent is that the aggregation effect is significant. For cyanobacteria, the most significant increase effect appeared at the inlet area in August. The difference occurred in the water area near the outlet in September and October. For diatoms, and similarly with cyanobacteria, the increase was first observed in the inlet area and then moved to the downstream area of the grass sandbar. However, for chlorophyta and cryptophyta, the biomass increase seems to be equally distributed throughout the entire reservoir, even without differences between months.

To summarize, the patterns were slightly different in the reservoir as a whole. The lower part of the reservoir represented the more common pattern of the phytoplankton community than that observed at the entrance and in the region around the Grass Sandbar. In addition, the

aggregation area of phytoplankton changed during the transition period.

5 Discussion

5.1 Common phytoplankton community patterns in the Qingcaosha Reservoir

As described above, the most obvious characteristic in the common pattern of the phytoplankton community in the Qingcaosha Reservoir is the existence of two temporal periods: late summer to autumn and winter to early spring. In addition, the species composition varies by time period. Although the number of species is smaller than other phyla, cyanobacteria dominate during late summer and autumn. However, cyanobacteria are barely detected during winter and early spring when chlorophyta, diatoms and cryptophyta are dominant. Finally, the patterns of phytoplankton in different regions of the Qingcaosha Reservoir show strong homogeneity with little variation between the entrance and lower parts.

Referring to the relevant literature and local environmental characteristics, an attempt was made to identify the possible cause of this pattern in the Qingcaosha Reservoir. A subtropical monsoon climate and clear distinction between seasons directly led to the main pattern of the phytoplankton community in the reservoir. The field measurements executed by the Shanghai Controlling and Monitoring Center of Water Supply in July and August

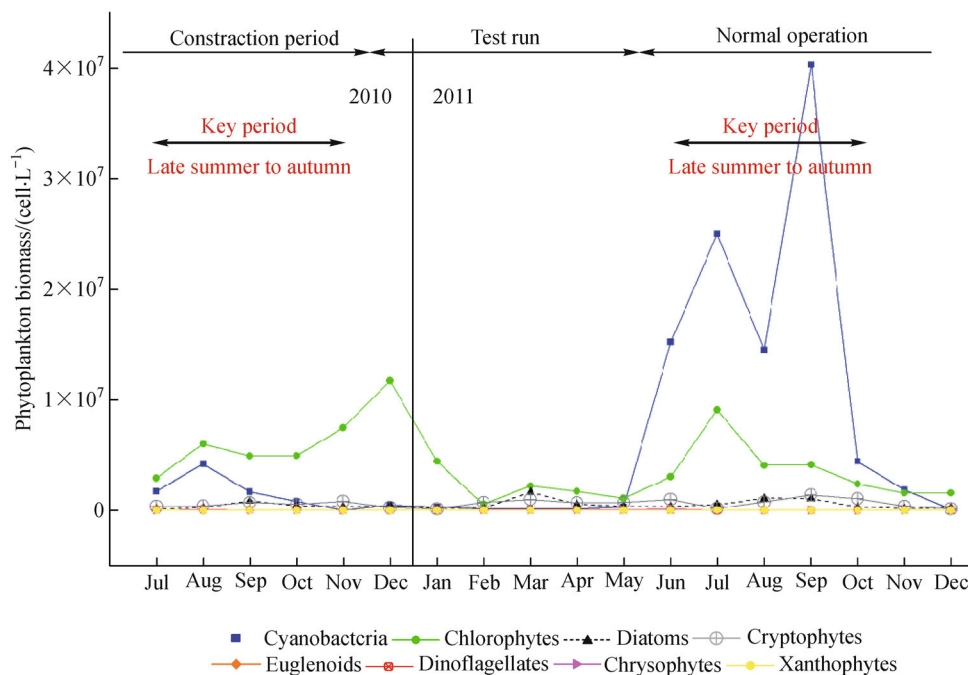


Fig. 6 GIS-based phytoplankton biomass distribution changes between 2010 and 2011 (August to October).

show that the water temperature fluctuated from 25°C to 30°C and that the light intensity near the surface fluctuated from 11,900 to 171,410 lux. This high temperature corresponded to the maximum growth rate of most cyanobacteria (Robarts and Zohary, 1987). Regarding light intensity, most research has suggested that cyanobacteria are sensitive to prolonged periods of intense light and that light intensities higher than 17,777 lux ($320 \mu\text{E}\cdot\text{m}^{-2}\cdot\text{s}^{-1}$) were even lethal for some species (van Liere and Mur, 1979). However, the local climate of Qingcaosha was characterized as both marine and monsoon with high amounts of rainfall and typhoons during summer and autumn. These precipitation events broke the long period of high light intensity with several cloudy days. This intermittent exposure to sunlight allows cyanobacteria to grow near their maximal rate. Additionally, the optimum temperatures of chlorophyta and diatoms are lower than those of cyanobacteria. For instance, the growing rates of diatoms and chlorophyta reach two to four times that of most cyanobacteria at 20°C (van Liere and Walsby, 1982). The dominance of cyanobacteria then decreases as chlorophyta, diatoms and cryptophyta take advantage of the relatively low temperature. The combined action of these factors may have promoted the growth of cyanobacteria. Given the complicated combined action of the factors, further study can reinforce the initial selection of significant parameters and the reasoning analysis (Chau and Muttil, 2007). In similar case studies, statistical analysis methods were applied to the criteria selection, such as Artificial Neural Network and Multiple Criteria Data Envelopment Analysis (Wu and Chau, 2006; Xie et al., 2006; Zhao et al., 2006). Using this method, the interrelationship between population pattern and the selected criteria could then be promoted.

Because the Qingcaosha Reservoir was constructed as an east-west elongated, fusiform reservoir, the north dam (one long edge) is approximately 20 km long, while the circumference of the reservoir is 48.79 km. The only intake sluice was constructed at the upstream end, and two outlet sluices were constructed at the downstream end. During the non-saltwater period, the Yangtze River flows into the reservoir while the intake sluice is open. After being parted by the Grass Sandbar, water flows to the downstream end of the reservoir. The changes in the phytoplankton community structure are in accordance with this process. The elongated reservoir lengthens the time it takes for water to flow through. This longer progress slows the flow rate and decreases the nutrient concentration. The weakening of the physical disturbance of the deep water column is thought to influence the growth of phytoplankton more significantly than nutrient and light intensity (Havens et al., 2003; Figueredo and Giani, 2009). Moreover, in wastewater treatment research, it was discovered that the biomass of phytoplankton is reduced when it flows through higher wetland plant communities. The Grass Sandbar, which features dense vegetation, is in the middle

of the reservoir. *Phragmites australis* and *Solidago decurrens* are the primary plants on the Grass Sandbar, and their dense stems and surrounding soil contribute to the change in the phytoplankton community. Thus, the community structures in the narrow upper part of the reservoir differ from those in the compromise and the lower part.

5.2 Differences in the phytoplankton community between 2010 and 2011

Monthly sampling was conducted beginning in July 2010, six months before the regular operation of the reservoir. The seven-month dataset covered the summer and autumn seasons, the time period when the cyanobacteria were most likely to bloom. This allowed for a comparative analysis for the summer and autumn months of 2010 and 2011. The biomass, number of species, and spatial distribution can be compared on a year-to-year basis to obtain the variation tendency of the phytoplankton community.

There was an increasing trend over time of phytoplankton biomass (Fig. 7). The average biomass in 2011 was much larger than that in 2010. The average biomass from July to October 2010 was above 7.7×10^6 cells/L, whereas in 2011, it was 2.8×10^7 cells/L. Moreover, compared with 2010, the cyanobacteria biomass rapidly increased in the summer of 2011, while the chlorophyta biomass showed little change. As some filamentous cyanobacteria can form reproductive spores under severe conditions and some species, such as *Microcystis* spp., spend winter dormant on the sediment surface, the accumulation of cyanobacteria in 2010 provided a higher incipient cell concentration in 2011. Other research also showed that cyanobacteria are typically the dominant phylum in both marine and freshwater systems (Dokulil and Teubner, 2000; Quiblier et al., 2008). It is appropriate to say that cyanobacteria will become the dominant phylum in the reservoir after regular operation.

In regard to spatial distribution, the GIS-based assessment showed an obvious change in phytoplankton aggregation. The trend that the aggregation area was moving downstream warned of a higher risk of algal bloom in the following operation. The consistent changes in the four months and in all of the phyla exclude the sampling error as the reason for the change. This may be due to the residual spores or the nutrients that had accumulated in the sediment.

The dominant species changed over the two years of the study, especially in the summer. From June to August 2010, the dominant species in the Qingcaosha Reservoir were chlorophyta and cryptophyta, including the species of *Chlorella vulgaris*, *Ulothrix* spp., *Scenedesmus* spp., and *Chroomonas acuta*. In all families, chlorophyta were dominant in both biomass and the number of species. However, the dominant family in the summer of 2011 was cyanobacteria with merely four species. The most

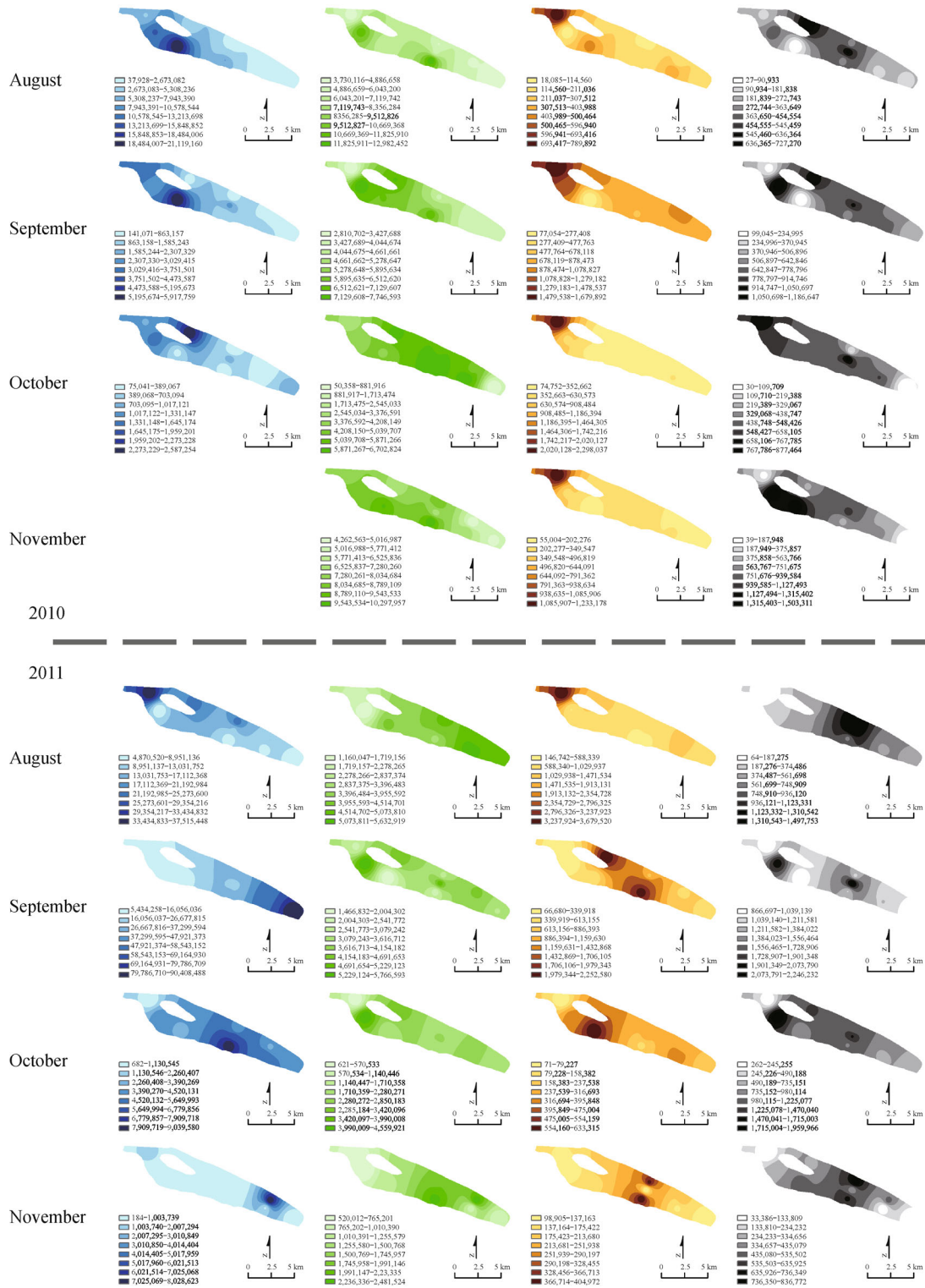


Fig. 7 Comparison between the phytoplankton biomass of different phyla in 2010 and 2011.

dominant species was *Microcystis* spp., whereas chlorophyta, with a larger number of species, had a limited dominance.

The degree of dominance also changed after the change in the water supply. The dominant species (*Scenedesmus bijuga*) in July 2010 had a Y of 0.11; whereas the subdominant species (*Chlorella vulgaris*) had a Y of 0.07. However, in the corresponding period in 2011, Y was 0.81 for the dominant species (*Microcystis* spp.) with only 0.10 and 0.07 for *Chlorella vulgaris* and *Phormidium tenne* (the subdominant species), respectively. *Microcystis* spp. monopolized the dominance. In other words, the differences in the degree of dominance between the species were small in 2010, but large in 2011.

5.3 Suggestions for reservoir monitoring and management

The average biomass and high concentration of phytoplankton observed in summer and autumn of 2011, near the water outlet in the lower areas of Qingcaosha Reservoir, indicated a potential risk of algal bloom. Given the reservoir intakes water from the bottom, the flow rate of the surface water would be slower. This longer water resistance time at the surface provides ideal conditions for phytoplankton productivity. Additionally, the prevailing winds come from the southeast during summer, which contrast with the direction of the reservoir's water flow, thus impeding the flow rate of the surface water. Moreover, the coastal waters could be vulnerable to eutrophication due to the accumulation of nutrients in the sediments (Chau and Muttil, 2007) increasing the risk of cyanobacteria in the near future. One common solution would be to enhance the frequency of the water exchange. The distribution of the Yangtze River runoff presents obvious seasonal variation. The majority of the runoff, which includes 71.3% of the overall discharge in one year, occurs from May to October, whereas the dry season contributes 28.7% of the overall discharge. This discharge will, to a certain degree, counteract the adverse wind and the aggregation of phytoplankton.

However, there is also a possible risk that phytoplankton populations will increase due to the updated water. When water exchange is executed, the assembled phytoplankton will be expelled. However, on the other hand, the upstream waters and water from the estuary would be brought into the reservoir and the amount of phytoplankton would increase. Moreover, the water flow would disturb the silt in the reservoir, consequently reactivating the nutrients in the silt, such as ammonium, nitrate, and phytoplankton, as was assumed in similar studies (Malone et al., 1988; Calijuri et al., 2002; Cornelisen and Thomas, 2006). This possibility should be researched in a future study.

It can be concluded then that consistent monitoring of phytoplankton and water quality within the reservoir is essential to effectively guide management actions. However, long-term, regular monitoring of the entire reservoir

area consumes considerable human and fiscal resources. Additionally, there may be a time cost for issuing the state of phytoplankton and the bloom risk grade. From the study results, it is appropriate to simplify and rebuild the regular monitoring plan. First, reduce the number of species monitored from all that are visible to only those representative based on biomass and dominance. A maximum number of species could initially be included in this study, decreasing to a limited number by the end. Cyanobacteria observed from summer to autumn and diatoms in winter should be monitored particularly carefully. The monitoring frequency should then be separated into two periods: late summer to autumn (July to October) and then for the remainder of the year. In late summer to autumn, weekly or even daily sampling is necessary. In contrast, monthly monitoring is appropriate during other times of the year. Finally, the monitoring area should be confined to the lower part of the reservoir where the sampling stations should be of primary concern for management. Stations near the upper sluice should be reduced to one or two to represent the initial state of water in the reservoir.

6 Conclusions

The integrated assessment method in which statistical analysis can work in concert with GIS-based assessment can show a clear temporal-spatial distribution pattern in large-area reservoirs or lakes. After the calculation, a GIS assessment can test the statistical results and display the general pattern and special case. This method was applied to Qingcaosha Reservoir and the following results were concluded.

During the transition period, the phytoplankton population pattern has two main characteristics in the reservoir: 1) late summer to autumn is characterized by the monopolistic dominance of cyanobacteria, and 2) winter to early spring is characterized by the dominance of both chlorophyta and diatoms. Small differences exist between the upper and lower parts. The phytoplankton biomass increased sharply after the regular operation of the reservoir, and the dominant species become monopolistic. Cyanobacteria experienced a dramatic increase in summer 2011, and the cell concentration indicated a risk of blooming. It is also suggested that a regular monitoring with higher efficiency could focus on stations in the lower part of the reservoir and on several species.

The present research reveals the initial phytoplankton population pattern and demonstrates the need for regular monitoring of the Qingcaosha Reservoir. The study analyzed monitoring data from the time period of 2010 to 2011. However, it could be improved by considering the population of phytoplankton after the regular operation, the effect of water quality and other environmental factors with more sufficient data from related research. Further

study should focus on the effect of the operation on phytoplankton and changes in the environment. Additionally, the long-term, regular phytoplankton pattern and environmental controls of phytoplankton growth could be particularly useful in the water management of coastal reservoirs, especially in the subtropics.

Acknowledgements This work was funded and supported by the National Natural Science Foundation of China (Grant No. 71073055) and the Science and Technology Commission of Shanghai Municipality (09DZ120010A). Lin Ma and Xiaoyu Zheng are acknowledged for their help with monitoring samples, and Haiying Zhang, Meng Wu, Sheng Xie, and Yan Jin are acknowledged for their help with the sampling. We are indebted to Xin Tong for guidance regarding R software. We are also grateful to Professor Yongjie Gu for her work in the field survey and her support in the identification of the phytoplankton.

References

- Bartram J, Carmichael W, Chorus I, Jones G, Skulberg O (1999). Toxic cyanobacteria and other water-related health problems. In: Chorus I, Bartram J, eds. *Toxic Cyanobacteria in Water: A Guide to Their Public Health Consequences, Monitoring and Management*. London: E&FN Spon, 17–20
- Bertrand F, Maumy M (2010). Using partial triadic analysis for depicting the temporal evolution of spatial structures: assessing phytoplankton structure and succession in a water reservoir. *Case Studies in Business, Industry & Government Statistics*, 4(1): 23–43
- Calijuri M C, Dos Santos A C A, Jati S (2002). Temporal changes in the phytoplankton community structure in a tropical and eutrophic reservoir (Barra Bonita, S.P.—Brazil). *J Plankton Res*, 24(7): 617–634
- Carassou L, Ponton D (2006). Spatio-temporal structure of pelagic larval and juvenile fish assemblages in coastal areas of New Caledonia, southwest Pacific. *Mar Biol*, 150(4): 697–711
- Carlson R (1977). A trophic state index for lakes. *Limnol Oceanogr*, 22(2): 361–369
- Chau K, Muttill N (2007). Data mining and multivariate statistical analysis for ecological system in coastal waters. *Journal of Hydroinformatics*, 9(4): 305–317
- Chen Y, Fan C, Teubner K, Dokulil M (2003a). Changes of nutrients and phytoplankton chlorophyll-a in a large shallow lake, Taihu, China: an 8-year investigation. *Hydrobiologia*, 506–509(1–3): 273–279
- Chen Y, Fan C, Teubner K, Dokulil M (2003b). Long-term dynamics of phytoplankton assemblages: *Microcystis*-domination in Lake Taihu, a large shallow lake in China. *J Plankton Res*, 25(4): 445–453
- Chen Y, Liu R, Sun C, Zhang P, Feng C, Shen Z (2012). Spatial and temporal variations in nitrogen and phosphorous nutrients in the Yangtze River Estuary. *Mar Pollut Bull*, 64(10): 2083–2089
- Cornelisen C D, Thomas F I M (2006). Water flow enhances ammonium and nitrate uptake in a seagrass community. *Mar Ecol Prog Ser*, 312: 1–13
- Dai Z, Du J, Zhang X, Su N, Li J (2011). Variation of riverine material loads and environmental consequences on the Changjiang (Yangtze) Estuary in recent decades (1955–2008). *Environ Sci Technol*, 45(1): 223–227
- Dokulil M T, Teubner K (2000). Cyanobacterial dominance in lakes. *Hydrobiologia*, 438(1/3): 1–12
- Downing J A, Watson S B, Mccauley E (2001). Predicting cyanobacteria dominance in lakes. *Can J Fish Aquat Sci*, 58(10): 1905–1908
- Dudgeon D (2000). Large-scale hydrological alterations in tropical Asia: prospects for riverine biodiversity. *Bioscience*, 50(9): 793–806
- Figueredo C C, Giani A (2009). Phytoplankton community in the tropical lake of Lagoa Santa (Brazil): conditions favoring a persistent bloom of *Cylindrospermopsis raciborskii*. *Limnologia*, 39(4): 264–272
- Gaertner J C (2000). Seasonal organization patterns of demersal assemblages in the Gulf of Lions (north-western Mediterranean Sea). *J Mar Biol Assoc U K*, 80(5): 777–783
- Garant D, Kruuk L E B, Wilkin T A, McCleery R H, Sheldon B C (2005). Evolution driven by differential dispersal within a wild bird population. *Nature*, 433(7021): 60–65
- Havens K E, James R T, East T L, Smith V H (2003). N: P ratios, light limitation, and cyanobacterial dominance in a subtropical lake impacted by non-point source nutrient pollution. *Environ Pollut*, 122(3): 379–390
- Hunt R J, Matveev V F (2005). The effects of nutrients and zooplankton community structure on phytoplankton growth in a subtropical Australian reservoir: an enclosure study. *Limnologia*, 35(1–2): 90–101
- Karadžić V, Subakov-Simić G, Krizmanić J, Natić D (2010). Phytoplankton and eutrophication development in the water supply reservoirs Garaši and Bukulja (Serbia). *Desalination*, 255(1–3): 91–96
- Kummu M (2009). Water management in Angkor: human impacts on hydrology and sediment transportation. *J Environ Manage*, 90(3): 1413–1421
- Legendre P, Fortin M (1989). Spatial pattern and ecological analysis. *Vegetatio*, 80(2): 107–138
- Maier G, Glegg G A, Tappin A D, Worsfold P J (2012). A high resolution temporal study of phytoplankton bloom dynamics in the eutrophic Taw Estuary (SW England). *Sci Total Environ*, 434: 228–239
- Malone T C, Crocker L H, Pike S E, Wendler B W (1988). Influences of river flow on the dynamics of phytoplankton production in a partially stratified estuary. *Mar Ecol Prog Ser*, 48: 235–249
- Muttill N, Chau K (2006). Neural network and genetic programming for modelling coastal algal blooms. *Int J Environ Pollut*, 28(3/4): 223–238
- Muttill N, Chau K (2007). Machine learning paradigms for selecting ecologically significant input variables. *Eng Appl Artif Intell*, 20(6): 735–744
- Pan G, Yang B, Wang D, Chen H, Tian B, Zhang M, Yuan X, Chen J (2011). In-lake algal bloom removal and submerged vegetation restoration using modified local soils. *Ecol Eng*, 37(2): 302–308
- Pavoine S, Blondel J, Baguette M, Chessel D (2007). A new technique for ordering asymmetrical three-dimensional data sets in ecology. *Ecology*, 88: 512–523
- Pinckney J L, Paerl H W, Tester P, Richardson T L (2001). The role of nutrient loading and eutrophication in estuarine ecology. *Environ Health Perspect*, 109(s5): 699–706
- Pringle C M (2001). Hydrologic connectivity and the management of

- biological reserves: a global perspective. *Ecol Appl*, 11(4): 981–998
- Quiblier C, Leboulanger C, Sané S, Dufour P (2008). Phytoplankton growth control and risk of cyanobacterial blooms in the lower Senegal River delta region. *Water Res*, 42(4–5): 1023–1034
- Ren H, Zhang P, Liu C, Xue Y, Lian B (2010). The potential use of bacterium strain R219 for controlling of the bloom-forming cyanobacteria in freshwater lake. *World J Microbiol Biotechnol*, 26(3): 465–472
- Robarts R D, Zohary T (1987). Temperature effects on photosynthetic capacity, respiration, and growth rates of bloom-forming cyanobacteria. *N Z J Mar Freshw Res*, 21(3): 391–399
- Robert P, Escoufier Y (1976). A unifying tool for linear multivariate statistical methods: the RV-coefficient. *Appl Stat*, 25(3): 257–265
- Roberts J J, Best B D, Dunn D C, Trembl E A, Halpin P N (2010). Marine geospatial ecology tools: an integrated framework for ecological geoprocessing with ArcGIS, Python, R, MATLAB, and C++. *Environ Model Softw*, 25(10): 1197–1207
- Rolland A, Bertrand F, Maumy M, Jacquet S (2009). Assessing phytoplankton structure and spatio-temporal dynamics in a freshwater ecosystem using a powerful multiway statistical analysis. *Water Res*, 43(13): 3155–3168
- Rossi J P (2003). The spatiotemporal pattern of a tropical earthworm species assemblage and its relationship with soil structure. *Pedobiologia (Jena)*, 47: 497–503
- Schindler D W (1977). Evolution of phosphorus limitation in lakes. *Science*, 195(4275): 260–262
- Shanghai Water Authority (2009). Shanghai water resource bulletin, 2009. http://www.shanghaiwater.gov.cn/web/sw/2009_1_1.jsp. 2012, 10, 27
- Smith V H (1983). Low nitrogen to phosphorus ratios favor dominance by blue-green algae in lake phytoplankton. *Science*, 221(4611): 669–671
- Soares M C S, Marinho M M, Azevedo S M O F, Branco C W C, Huszar V L M (2012). Eutrophication and retention time affecting spatial heterogeneity in a tropical reservoir. *Limnologica*, 42(3): 197–203
- Thomas L, Buckland S T, Rexstad E A, Laake J L, Stringberg S, Hedley S L, Bishop J R B, Marques T A, Burnham K P (2010). Distance software: design and analysis of distance sampling surveys for estimating population size. *J Appl Ecol*, 47(1): 5–14
- van Liere L, Mur L R (1979). Growth Kinetics of *Oscillatoria agardhii* gomont in continuous culture, limited in its growth by the light energy supply. *J Gen Microbiol*, 115(1): 153–160
- van Liere L, Walsby A E (1982). Interactions of cyanobacteria with light. In: Burnett J H, Baker H G, Beevers H, Whatley F R, eds. *The Biology of Cyanobacteria*. Oxford: Blackwell, 9–45
- Wu C, Chau K (2006). Mathematical model of water quality rehabilitation with rainwater utilization — A case study at Haigang. *Int J Environ Pollut*, 28(3/4): 534–545
- Xie J, Cheng C, Chau K, Pei Y (2006). A hybrid adaptive time-delay neural network model for multi-step-ahead prediction of sunspot activity. *Int J Environ Pollut*, 28(3/4): 364–381
- Zeng H, Song L, Yu Z, Chen H (2007). Post-impoundment biomass and composition of phytoplankton in the Yangtze River. *Int Rev Hydrobiol*, 92(3): 267–280
- Zhao M, Cheng C, Chau K, Li G (2006). Multiple criteria data envelopment analysis for full ranking units associated to environment impact assessment. *Int J Environ Pollut*, 28(3/4): 448–464